ORIGINAL PAPER

Multi-scale characteristics of drought propagation from meteorological to hydrological phases: variability and impact in the Upper Mekong Delta, Vietnam

H. V. T. Minh[1] · P. Kumar[2] · N. K. Downes[1] · N. V. Toan[3] · G. Meraj[4] · P. C. Nguyen[5] · K. N. Le[6] · T. V. Ty[7] · K. Lavane[8] · R. Avtar[9,10] · M. Almazroui[11]

Abstract

The Vietnamese Mekong Delta (VMD) is highly vulnerable to drought, particularly in the context of climate change. Prolonged drought during the dry season has emerged as a significant natural disaster, severely affecting agriculture and socioeconomic development in the region. To enhance water resource management and agricultural productivity, this study examines the characteristics of meteorological droughts using the Standardized Precipitation Index (SPI) and the Standardized Precipitation Evapotranspiration Index (SPEI) in the upper Mekong Delta of Vietnam. The Mann–Kendall (MK) test and Sen's slope were employed to assess trends in drought and hydrological conditions. The results reveal no significant trends in rainfall, while average temperatures have increased significantly in most months, especially during the dry season. Although water levels and discharge at the Tan Chau and Chau Doc stations have decreased, significant reductions were primarily observed at Chau Doc station from 2000 to 2021. These findings provide critical insights for sustainable water resource management and planning in the VMD, considering future climate variability and changes in hydrological regimes.

1 Introduction

There is irrefutable evidence that climate change is advancing at an unprecedented rate (Ogunbode et al. 2020; Amatya and Khan 2023). Globally, rising sea surface temperatures are driving significant increases in air temperatures, as well as the frequency and intensity of extreme events such as droughts, floods, and heavy storms (Danandeh Mehr and Vaheddoost 2020; Minh et al. 2022a, b). The Multiple Climate Hazard Index ranks Southeast Asia as one of the most vulnerable regions to climate change (Yusuf and Francisco 2009), indicating that tropical regions are more sensitive and vulnerable to climate change. This increased vulnerability is largely due to elevated temperatures, which lead to higher evaporation rate (Vicente-Serrano et al. 2010). A study by Zeppel et al. (2008) found that

---

Extended author information available on the last page of the article

annual evaporation and transpiration can consume up to 80% of rainfall when annual rainfall is less than 1000 mm.

While a number of studies have attributed droughts, particularly in tropical and subtropical regions, primary to climate change (Lee and Dang 2019, Ropelewski and Halpert 1986; Roeckner et al. 1996; Vicente-Serrano et al. 2011), the influence of El Niño-Southern Oscillation (ENSO) phenomenon as a key driver of drought patterns has also been extensively documented (Roeckner et al. 1996; Food and Agriculture Organization (FAO) 2016; Lam et al. 2019; Minh et al. 2022a; Nguyen et al. 2023). Regions such as Australia, Southeast Asia, South Africa, and northern South America particularly susceptible to drought during El Niño events, and experience increased precipitation during La Niña events (Smith and Ropelewski 1997; Vicente-Serrano et al. 2011; Shehu et al. 2016). Moreover, the impact of ENSO extends beyond these regions, influencing weather patterns across the Pacific Ocean, North America, Europe, and parts of Central Asia (Diaz et al. 1992).

Several studies identified that ENSO was the main source of atmospheric circulation variability on a global scale that affects the water resources of the basin (Chandimala and Zubair 2007; Abtew et al. 2009). Chiew and McMahon (2002) examined the global teleconnection between ENSO and streamflow patterns by analyzing data from 581 catchments. A significant correlation between ENSO phases and streamflow variability was found across large geographical regions. The MRB has experienced significant inter-annual fluctuations in water availability, oscillating between severe droughts and major floods in recent decades. While climate change is generally recognized as a primary driver of these extremes, the influence of the ENSO phenomenon on regional hydrology is also evident (Nguyen et al. 2023). Moreover, other studies also confirmed a stronger relationship between ENSO and river discharge during the 1930s, 1940s, the1960s and 1970s at Vientiane and Pakse stations in the MRB (Darby et al. 2013; Räsänen and Kummu 2013).

Drought is typically categorized into three primary types based on deficiencies within the hydrological cycle: meteorological drought, characterized by a deficit in precipitation (below normal precipitation); agricultural drought below normal soil water levels), which is reflecting inadequate soil moisture; and hydrological drought, which is indicated by reduced river flows (below normal river flow) (Tallaksen and van Lanen 2004; Van Loon and Van Lanen 2013; Van Loon et al. 2016). Drought propagation varies by region, depending on climate, watershed, and human activity (Van Loon and Van Lanen 2013). Drought severity is a crucial indicator of drought impact (Hayes et al., 2010). To quantify severity, various standardized indices, such as the Standardized Precipitation Index (SPI) and the Standardized Precipitation Evapotranspiration Index (SPEI), Standardized Streamflow Index (SSI) have been employed in numerous studies (Van Loon and Laaha 2015; Wu et al. 2018; Zalokar et al. 2021; Minh et al. 2024a). Several scholars have revealed that precipitation is the main variable determining the onset, severity, duration, intensity, and termination of droughts (Heim 2002). SPI has been widely used for drought monitoring and analysis because to their simplicity and low data needs (Mishra and Singh 2010; Gumus et al. 2021). SPI responds differently to soil moisture, river discharge, reservoir storage, vegetation activity, agricultural yield, and land use changes (Szalai et al. 2000; Sims et al. 2002; Ji and Peters 2003; Vicente-Serrano 2006; Khan et al. 2008). Moreover, to be useful for drought monitoring and water resource management applications, indices must be associated with a specific time scale.

The main criticism of the SPI is that its calculation is based only on precipitation data. Whilst precipitation is a key predictor of the water supply, temperature, evapotranspiration, wind speed, and soil water holding capacity are also crucial variables that affect

overall water supply since they regulate the rate of evapotranspiration (Vicente-Serrano et al. 2010). Signs of drought can be derived from trends in variables, such as rainfall and temperature (Tirivarombo et al. 2018). However, the SPI is deficient when considering the impact of temperature on drought conditions, which strongly impacts the overall water balance at a regional scale. Vicente-Serrano et al. (2010) developed the SPEI based on precipitation and temperature data as an improved drought index that is particularly suited for studies of the effects of global warming on drought severity. In this regard, SPEI is an extension of SPI that considers the effects of temperature variability when assessing drought, as it employs a climatic water balance, or the difference between precipitation and reference evapotranspiration ($P—ET_0$), as the input (Beguería et al. 2014). Tirivaromno et al. (2018) found that the SPI exhibits the capacity to detect extreme droughts, whereas the SPEI has the strength to detect moderate to severe drought.

The SSI quantifies hydrological severity by transforming streamflow data into a standardized normal distribution associated with SPI. This approach allows for the identification of high and low flow periods, corresponding to flood and drought conditions, respectively. Some studies have employed the SSI to identify and assess the severity, duration, and frequency of droughts and floods (Wu et al. 2018; Minh et al. 2022a; Li et al. 2024b) or examine the influence of climate change and human activities on streamflow regimes (Wu et al. 2018; Naderi et al. 2022). Kimmany et al. (2024) investigated hydro-meteorological droughts in the Chao Phraya River Basin using the SSI, the study contributes to a deeper understanding of drought characteristics, including their frequency, duration, and severity (Kimmany et al. 2024). For example, Kang and Sridhar (2024) has also quantified the severity, duration, and frequency of droughts in different regions of the Mekong Basin. The SSI can be applied to longer time series, ranging from 1 to 12 months, to comprehensively capture cumulative water deficits and better understand the evolution of hydrological droughts (Nalbantis and Tsakiris 2009). It can be noted that this index has been widely adopted in hydrological studies to assess drought severity, duration, and frequency, aiding in water resources management, flood control, and disaster preparedness (Singh et al. 2022; Kang and Sridhar 2024).

For drought warnings to be effective, it is important to have a system for classifying drought severity, that is, missing water volumes from very low river flow or low rainfall. Polong et al. (2019) classified drought events using identical thresholds for the SPEI and SPI, regardless of the existing conflict. However, some authors have proposed different thresholds for the SPI and SPEI (Danandeh Mehr and Vaheddoost 2020). In addition, SPEI has been used in a wide variety of drought monitoring studies (Fuchs et al. 2012). Several of these studies reported that the SPEI correlated better with hydrological and ecological variables than other drought indices. Numerous studies have analyzed drought variability in Turkey (Partal and Kahya 2006; Danandeh Mehr and Vaheddoost 2020), as well as in other nations (Paulo et al. 2012; Potop et al. 2012; Sohn et al. 2013); the effect of drought atmospheric mechanisms (Boroneant et al. 2011), climate change (Krall et al. 2013); and agricultural practices (Potop et al. 2012). Using parametric and nonparametric methods, (Xu et al. 2003) investigated the potential long-term precipitation patterns in Japan. The majority of severe drought events are related to El Niño episodes (Quang et al. 2021, pp. 1985–2018), which is particularly true for Vietnam, including VMD (Tran et al. 2022).

Vujica M. Yevjevich developed the run theory in 1967 to objectively analyze sequences in time series data. The method focuses on identifying "runs," which are consecutive periods where data points consistently fall above or below a certain threshold (Yevjevich 1967). In studies on drought, this threshold usually signifies critical levels of precipitation or stream flow (Moyé et al. 1988; Şen 1989; Panu and Sharma 2002). These levels are

crucial for identifying and characterizing drought events (Ma et al. 2023). When studying droughts, run theory is useful for identifying when droughts begin and end, as well as for quantifying their severity and duration (Cancelliere and Salas 2004; Hao and Singh 2015; Gan et al. 2024). It also plays a crucial role in understanding how meteorological droughts, can lead to hydrological droughts (Li et al. 2024a). Effective drought risk assessment and management in the VMD relies on this understanding, enabling the development of strategies to mitigate drought impacts on water resources, agriculture, and communities.

The risk of disasters is rising in Vietnam, one of the most hydrometeorological hazard-prone countries in the Asia–Pacific region. Securing water resources and ensuring access to safe water for domestic use have become critical challenges across both urban and rural areas, especially in the face of increasing drought and saline intrusion (Dat 2020; Minh et al. 2024a).

The VMD in southwestern Vietnam accounts for 55.6% of the country's rice production (General Statistics Office of Vietnam (GSO) 2020), and is of great importance to the society, economy, and environment of the nation (Lavane et al. 2023; Minh et al. 2024c; Tri et al. 2004). However, drought and saline intrusion have both increased in magnitude and frequency in recent years owing to intensified upstream development (Binh et al. 2017). Consequently, drought monitoring, management, and mitigation are considered to be of high priority for both national and local governments. Considering its importance, this study investigates the spatio-temporal trends in the intensity, duration, and frequency of meteorological droughts over the VMD using SPI, SPEI and SSI. An Giang was selected as a case study due to its significance as a major food-producing province, contributing approximately 9.01% of the nation's total rice output and 16.1% of the VMDs rice production (GSO 2020).

Within An Giang (a province that represents the upper Mekong River region in Vietnam), the annual rainfall totals are below the average value of the Vietnam Meteorological and Hydrological Drought Index. Furthermore, there has been a decrease in the flow of the Mekong River in recent years. Drought conditions during the dry season have become increasingly common, posing significant threats to both life and livelihoods. In light of this knowledge gap, the present study aimed to assess the characteristics of drought and the meteorological variability of hydrological regimes as well as understand the meteorological and hydrological drought propagation characteristics in the study area in An Giang. To accomplish this goal, the SPI, SPEI and SSI were calculated for the multi-time series. The relationships between meteorological and hydrological propagations were conducted. The findings of this analysis were utilized to develop effective adaptation strategies that can be implemented in a timely manner to address drought conditions and promote sustainable water resource management and regional development.

2 Materials and methods

2.1 Study area and data collection

An Giang Province is situated in the western region of the VMD, bordered by the Mekong River (known locally as the Tien River) and the Bassac River (known as the Hau River). The province has a population of 2.4 million people. An Giang shares a 100-km-long northern border with Cambodia, and it is also bordered by Dong Thap Province to the east, Can Tho City to the south, and Kien Giang Province to the west (Fig. 1).
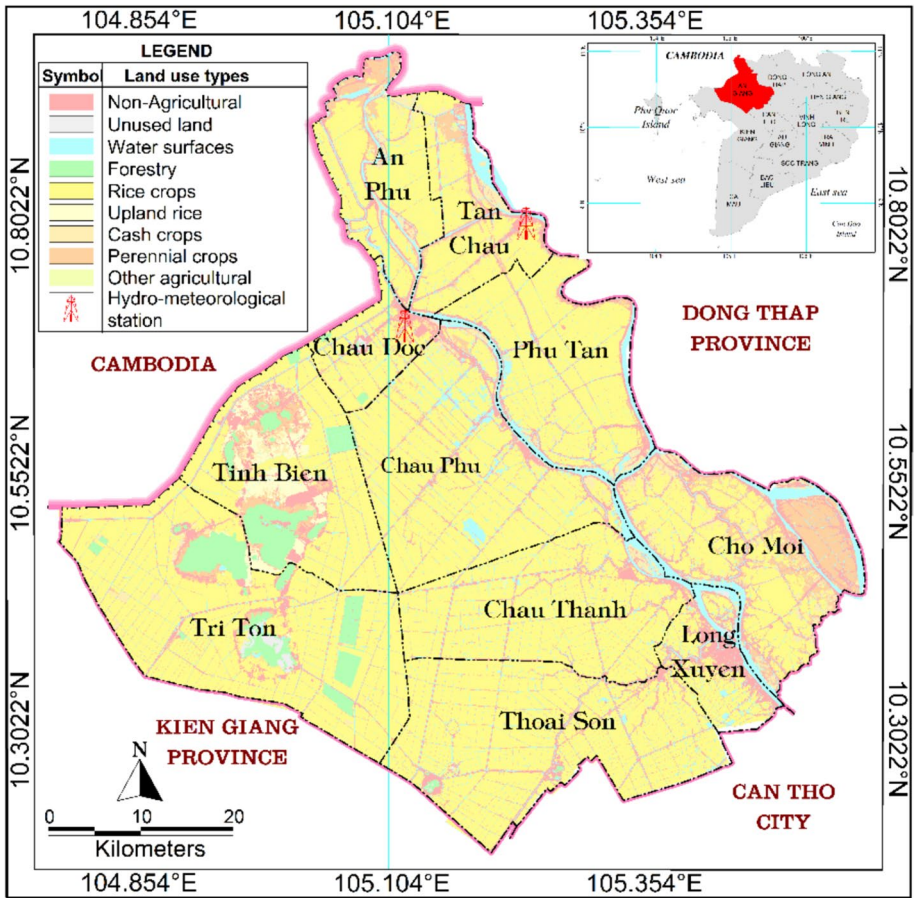
Fig. 1 Map highlighting and the location of An Giang Province with the Vietnamese Mekong Delta, including the hydro-meteorological stations of Tan Chau and Chau Doc

An Giang has two seasons, where the wet season spans from May to Nov while the dry season spans from Dec to Apr). The average annual rainfall and temperature were 1316 mm and 27.4 °C (1980–2021). For this period, the highest and lowest annual rainfall was 1920.9 mm (2008) and 691.5 mm (2002), respectively. The highest and lowest mean of annual temperatures were 26.6 °C (1991) and 28.1 °C (2020), respectively.

The monthly SPI and SPEI were calculated using hourly rainfall and temperature data (1980–2021) from the Chau Doc station. Daily water levels and discharges (2000–2021) at the Tan Chau and Chau Doc stations were collected. SPI, SSI, and SPEI threshold values for the estimated drought severity levels are shown in Table 1.

Table 1 Classification of drought conditions using SSI/SPI and SPEI indices

Classification	SSI/SPI thresholds	SPEI thresholds
Extremely wet	$SSI/SPI > 2$	$SPEI > 1.82$
Moderately wet	$1.5 < SSI/SPI \leq 2$	$1.42 < SPEI \leq 1.82$
Mildly wet	$1 < SSI/SPI \leq 1.5$	$1 < SPEI \leq 1.42$
Normal	$-1 < SSI/SPI \leq 1$	$-1 < SPEI \leq 1$
Mild drought	$-1.5 < SSI/SPI \leq -1$	$-1.42 < SPEI \leq -1$
Moderate drought	$-2 < SSI/SPI \leq -1.5$	$-1.82 < SPEI \leq -1.42$
Extreme drought	$SSI/SPI \leq -2$	$SPEI \leq -1.82$

2.2 Methods

2.2.1 SPI and SSI calculation

Precipitation-based drought indicators, such as the SPI, are founded on two premises: first, precipitation is significantly more variable than other factors, such as temperature and potential evapotranspiration (PET), and second, all the other variables remain stationary. SPI was used to define the periods of various time scales. Rainfall data should sum up the cumulative slip for both previous and current months with a slip equal to the duration of the drought. The conversion of these indicators resulted in the generation of drought indices that exhibited distinct attributes of drought. In this research, the time scales were assessed by utilizing the Standardized Precipitation Index (SPI) for the 3-, 6-, 9-, and 12-month periods.

SPI was developed by McKee et al. (1993) and is recommended by the World Meteorological Organization for monitoring and assessing meteorological drought. The density probability function for the Gamma distribution as shown in Eq. (1).

$$g(x) = \frac{1}{\beta^\alpha \Gamma(\alpha)} x^{\alpha-1} e^{-x/\beta} \tag{1}$$

where $\alpha > 0$ is the shape parameter, $\beta > 0$ is the scale parameter, $x > 0$ is the precipitation and the gamma function $\Gamma(\alpha)$ can be represented in Eq. (2).

$$\Gamma(\alpha) = \int_0^\infty y^{\alpha-1} e^{-y} dy \tag{2}$$

by using the Thom's approximation as shown in Eq. (3).

$$\hat{\alpha} = \frac{1}{4A}\left(1 + \sqrt{1 + \frac{4A}{3}}\right) \text{ and } \hat{\beta} = \frac{\bar{x}}{\hat{\alpha}} \tag{3}$$

where for n observations, $A = \ln(\bar{x}) - \frac{\sum \ln(x)}{n}$

The cumulative probability G(x) was obtained by integrating the density of the probability function g(x) with respect to x (Eq. 4).

$$G(x) = \int_0^x g(x)dx = \frac{1}{\hat{\beta}\Gamma(\hat{\alpha})} = \int_0^x x^{\hat{\alpha}-1} e^{\frac{-x}{\beta}} dx \tag{4}$$

Considering the limitation of the gamma function that is not defined by $x = 0$, and the possibility of zero precipitation, the cumulative probability becomes as shown in Eq. (5).

$$H(x) = q + (1-q)G(x) \tag{5}$$

where, q is the probability of zero precipitation. The SPI index was then obtained by transforming the cumulative probability into a normal standardized distribution with null average and unit variance (Eqs. 6 and 7).

$$Z = SPI = \begin{cases} -\left(t - \frac{c_0 + c_1 t + c_2 t^2}{1 + d_1 t + d_2 t^2 + d_3 t^3}\right), for\, 0 < H(x) \le 0.5, \\ +\left(t - \frac{c_0 + c_1 t + c_2 t^2}{1 + d_1 t + d_2 t^2 + d_3 t^3}\right), for\, 0.5 < H(x) \le 1 \end{cases} \tag{6}$$

$$t = \begin{cases} \sqrt{ln\left[\frac{1}{(H(x))^2}\right]}, for\ 0 < H(x) \le 0.5, \\ \sqrt{ln\left[\frac{1}{(1-H(x))^2}\right]}, for\ 0.5 < H(x) \le 1 \end{cases} \tag{7}$$

where $c_0 = 2.515517$, $c_1 = 0.802853$, $c_2 = 0.010328$; $d_0 = 1.432788$, $d_1 = 0.189269$, $d_2 = 0.001308$.

The methodology for calculating the SSI is similar to that of the Standardized Precipitation Index (SPI), with river discharge data substituted for rainfall data (Shamshirband et al. 2020).

2.2.2 SPEI calculation

The first step in calculating the *SPEI* was the estimation of *the PET*. Thereafter, the water balance equation was used to calculate deficit (D_i). Furthermore, P_i and PET_i are the precipitation and evapotranspiration over time i, respectively, and the difference D_i is between precipitation P_i and PET_i (Eq. 8). The cumulative climate water balance series for different time scales was established using Eq. (9).

$$D_i = P_i - PET_i \tag{8}$$

$$D_n^k = \sum_{i=0}^{k-1} \left(P_{n-i} - PET_{n-i}\right), n \ge k \tag{9}$$

where k and n are the time scale and the number of calculations, respectively. The formulas of the density function and cumulative probability function of the three-parameter log-logistic probability distribution are expressed in Eqs. (10 and 11) (Wang et al. 2015; Abbasi et al. 2019).

$$f(x) = \frac{\beta}{\alpha}\left(\frac{x-\gamma}{\alpha}\right)^{\beta-1}\left[1 + \left(\frac{x-\gamma}{\alpha}\right)^{\beta}\right]^{-2} \tag{10}$$

$$F(x) = \left[1 + \left(\frac{\alpha}{x-\gamma}\right)\right]^{-1} \tag{11}$$

where the parameters α, β, and γ are equal to the parameters of the scale, shape, and location for the D_i values in the range of $\infty < D < \gamma$. These were defined using the L-moment method (Eqs. 12–15).

$$\beta = \frac{2w_1 - w_0}{6w_1 - w_0 - 6w_2} \tag{12}$$

$$\alpha = \frac{(w_0 - 2w_1)\beta}{\Gamma\left(1 + \frac{1}{\beta}\right)\Gamma\left(1 - \frac{1}{\beta}\right)} \tag{13}$$

$$\gamma = w_0 - \alpha\Gamma\left(1 + \frac{1}{\beta}\right)\Gamma\left(1 - \frac{1}{\beta}\right) \tag{14}$$

where Γ is the gamma function of β and w_i $(i = 0, 1, 2...)$, which is computed by probability-weighted moments through the L-moment method (Hosking 1990).

$$w_1 = \frac{1}{n}\sum_{i=1}^{n} x_i\left(1 - \frac{i - 0.35}{n}\right)^i \tag{15}$$

where x_i and n are the ordered random sample and sample size, respectively. The probability distribution function is given by Eq. (16).

$$F(x) = \left[1 + \left(\frac{\alpha}{x - \gamma}\right)^\beta\right]^{-1} \tag{16}$$

The cumulative probability density was transformed into a standard normal distribution to obtain the corresponding *SPEI* time series of changes, as shown in Eq. (17).

$$SPEI = W - \frac{C_0 + C_1 W + C_0 W^2}{1 + d_1 W + d_2 W^2 + d_3 W^3} \tag{17}$$

where, $W = (-2\ln P)^{0.5}$, P is the probability of exceeding the determined moisture gain/loss, when $P \leq 0.5$, $P = 1 - F(x)$, when $P \geq 0.5$.

2.2.3 Run theory method

Run theory, introduced by Yevjevich (1967), is a valuable tool for analyzing time series data to identify and characterize drought events (Fig. 2). This method defines a drought as a continuous period during which an index (e.g., SPI, SSI) falls below a threshold, allowing for the quantification of drought severity, duration, frequency, and intensity (Li et al. 2017; Wu et al. 2019; Mesbahzadeh et al. 2020). In this study, drought events were defined as consecutive months with index values below − 1, with severity representing the cumulative deficit below a predefined threshold.

Drought severity is calculated as the sum of index values below the threshold, while duration represents the event's length; the frequency of drought is the number of events when the SPI and SSI values were below the threshold. The transition from meteorological to hydrological drought, termed PT, is determined by the time lag between the onset of these drought types (Wu et al. 2021) while Sattar et al. (2019) and Sattar et al. (2019)
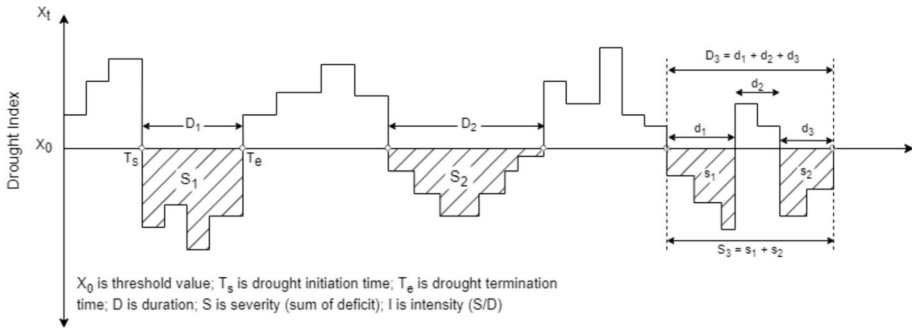
X₀ is threshold value; T_s is drought initiation time; T_e is drought termination time; D is duration; S is severity (sum of deficit); I is intensity (S/D)

Fig. 2 Identifying drought patterns through run theory analysis

use response rate (R_r) to quantify the propagation of meteorological drought to hydrologic In this study, the drought event (SPI and SSI) were defined as a consecutive sequence of months (t) with drought indices values less than a of -1 that was described by severity (S) which represents the cumulative deficit of a specific hydrological parameter below a predefined threshold. Drought initiation (T_s) marks the beginning of a drought event, while termination (T_e) signifies its end when water scarcity subsides. Drought duration (D) is calculated as the interval between these two points. Drought intensity (I) was determined by dividing the total drought deficit by the duration of the event.

If a drought event consists of two distinct periods (d_0 and d_2) separated by a short interruption (d_1) of less than six months and SPI (SSI) values ranging from 0 to 1, the event was deemed continuous. Therefore, the combined duration of the two drought periods (d_0, d_1, and d_2) was considered a single drought event (D_2), with its corresponding magnitude (S_2) determined by summing the magnitudes of the individual drought periods (s_1 and s_2) (Mitra and Srivastava 2017; Wu et al. 2018; Zhong et al. 2020).

To assessment the relationship between meteorological and hydrological droughts, we employed R_r to assess drought propagation rate and lag time. A higher of R_r indicated a stronger relationship between the two drought types, meaning hydrological drought was more sensitive to meteorological conditions. Conversely, a lower of R_r suggested a weaker connection. Lag time was calculated by determining the temporal offset between the onset of meteorological and hydrological droughts. The response rate and lag time were showed in Eqs. 18 and 19.

$$R_r = \frac{n}{m} \cdot 100\% \tag{18}$$

$$L_T = T_M - T_H \tag{19}$$

The R_r was represented as the percentage of hydrological drought events (n) that responded to meteorological drought events, out of the total number of meteorological drought events (m) during the study period. Lag time (L_T) was determined by calculating the time difference between the onset of meteorological drought (T_M) and the subsequent hydrological drought (T_H).

2.2.4 Mann Kendall test and sequential Mann–Kendall analysis

Parametric and non-parametric methods can be used to detect trends. Parametric approaches are powerful for normally distributed data (Bihrat and Bayazit 2003). However, as aforementioned, non–parametric approaches produce more reliable results in the case of hydrology and meteorology, and are more commonly conducted (Hirsch and Slack 1984; Hirsch et al. 1992). The MK test (Mann 1945) and Sen's slope (Sen 1968) are widely used non–parametric analyses for detecting trends in direction and magnitude of meteo–hydrological time series. In addition, Sequential Mann–Kendall (SMK) analysis was conducted to detect the starting point of trends (Esteban-Parra et al. 1995). This means that trend detection at the end of any time period using the MK does not provide a complete structure of the trend. There may be fluctuations in the trend over the investigation period, which can only be detected by sequentially applying the test for every individual period (Sneyers 1991).

Rank values were used to compute the SMK test. The ranked value y_i of the original values in the series$(x_1; x_2; x_3; \dots ; x_n)$, the magnitudes of $y_i (i = 1;2;3; \dots ;n)$ were compared with$y_j (j = 1;2;3; \dots ; i - 1)$. For each comparison, the cases where $y_i > y_j$ were counted and denoted byn_i. The statistic t_i, the distribution of test statistict_i, and variance are thus calculated (Eqs. 20–22).

$$t = \sum_{j=1}^{i} n_i \tag{20}$$

$$E(t_i) = \frac{i(i - 1)}{4} \tag{21}$$

$$VAR(t_i) = \frac{i(i - 1)(2i + 5)}{72} \tag{22}$$

The forward sequential values of the statistic $u(t_i)$ is then calculated using the following equation (Sneyers 1991) (Eq. 23)

$$u(t_i) = \frac{[t_i - E(t_i)]}{\sqrt{Var(t_i)}} \tag{23}$$

The backward sequential statistic, $u\prime(t_i)$ is estimated in the same manner but starting from the end of the series. This method has been employed by many researchers to detect the onset of trends (Esteban-Parra et al. 1995). Nalley et al., (2013) used the method to find time periodicities in temperature time series. In the present study, this method was applied to identify trend–turning points (Nalley et al. 2013), when the curves $u(t_i)$ and $u\prime(t_i)$ were plotted. The point of intersection of the curves $u(t_i)$ and $u\prime(t_i)$ identifies a recognized change of direction. A detectable change in the time series can be inferred if the intersection of $u(t_i)$ and $u\prime(t_i)$ occurs within 1.96 (5% level) of the standardized statistic.

3 Results

3.1 Rainfall and temperature variability analysis

Figure 3 shows the monthly anomalies at Chau Doc station. The findings indicate that while some months during the wet season experienced above-average rainfall, certain months in the dry season also recorded increased rainfall. However, these variations were not statistically significant at the 5% level. Chau Doc's average annual rainfall of 1321 mm was
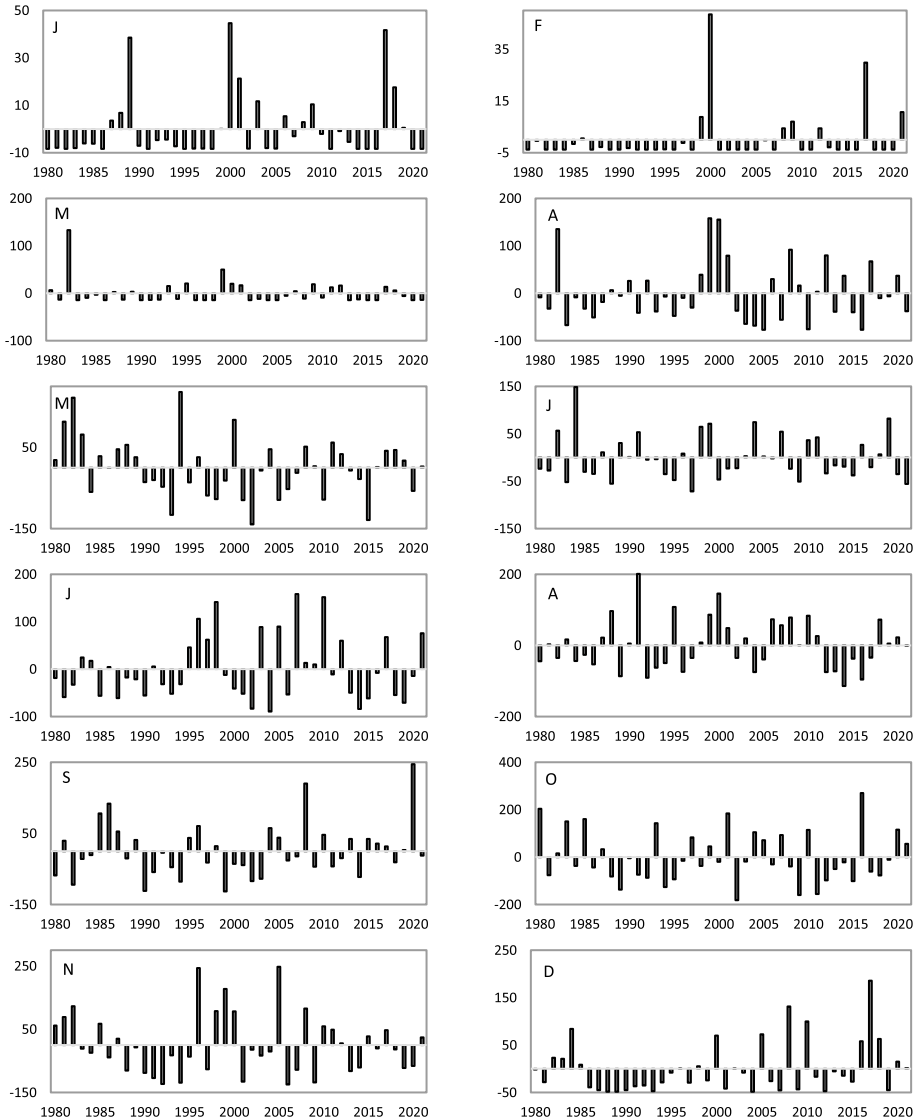

Fig. 3 The anomaly in monthly rainfall variability (1980–2021) at Chau Doc. J–D denotes January to December. X–axis denotes rainfall in mm and Y–axis denotes time in year

significantly lower than the Mekong Delta's regional average of 1695 mm (1980–2021), making it the area with the lowest annual rainfall in the VMD. The dry season (Dec to Apr) rainfall values were 48.376, 8.885, 3.983, 15.015, and 79.324 mm, respectively, which was characterized by minimal rainfall, with Jan and Feb recording the lowest averages. However, these typically drier months displayed higher rainfall variability compared to the remaining dry season months. Moreover, it is evident that monthly rainfall during the wet season has a lower coefficient of variation (CV) than that during the dry season, with CV values of 0.546 and 1.525, respectively. The average monthly rainfall during the wet season ranged from 120.96 mm to 269.67 mm, with Oct and Sept recording the highest amounts at 269.67 mm and 171.36 mm, respectively.

An Giang is located in a subtropical region of Southeast Asia, characterized by consistently high temperatures and humidity throughout the year. Given the significant influence of temperature on evapotranspiration rates, temperature was also employed to assess drought severity. Average temperatures in the study area were 27.8 °C during the dry season and 26.9 °C during the rainy season. Jan exhibited the lowest temperature at 25.8 °C, while Apr recorded the highest at 28.8 °C. Figure 4 shows the upward trend in average monthly temperatures at Chau Doc from 1980 to 2021.

The Mann–Kendall and Sen's slope tests were used to supplement the examination of monthly temperature anomalies, indicated significant upward temperature trends (Fig. 5 and Table 3). The Sen's slope analysis revealed significant increasing trends ($p < 0.05$) in average monthly temperatures for all months except Sept and Oct. The average rate of temperature increase, as determined by the Sen's slope analysis, was 0.26 °C per decade. May experienced the most rapid increase with a slope of 0.34 °C per decade, while Dec exhibited the slowest rate at 0.18 °C per decade. The SMK test was employed to quantify the magnitude and direction of trends in average monthly temperatures over the study period. The SMK testing was conducted to assess the statistical significance of these trends and estimate the timeframe for substantial temperature rises (Fig. 5).

The increasing trends in average monthly temperature typically occur earlier in the wet season than in the dry season. The dry season months of Dec, Jan, Feb, Mar, and Apr experienced increasing average temperatures starting in 1999, 2015, 2000, 2012 and 2012, respectively. These trends attained statistical significance from 2017, 2018, 2010, 2014 and 2015 onward for the corresponding months. The average temperatures for the wet season months of May, June, July, Aug, and Nov increased starting in the years 2014, 2007, 2019, 2005, and 2015, respectively. These increases became statistically significant starting in 2005, 2007, 2014, 2015, and 2019, respectively. The average monthly temperatures have increased statistically significantly since 2012 during the wet season and since 2014 during the dry season.

3.2 Drought analyses

SPIs and SPEIs were calculated for 3-, 6-, 9-, and 12-month timescales to graphically represent the temporal evolution of drought conditions (Figs. 6 and 7).

Figure 6a–d highlights fluctuating SPI values, indicative of alternating wet and dry periods. The only significant declining trends were identified in SPI-3 from 1983 to 1995, SPI 6 and SPI 9 from 1985 to 1995, and SPI 12 from 1985 to 1994 at the 95% confidence level using SMK. Mild drought events were the most prevalent, occurring 48, 30, 39, and 44 times for SPI 3-, 6-, 9-, and 12-month, respectively time scales, respectively. Moderate droughts were followed by occurrences of 20, 23, 27, and 24 events, while extreme
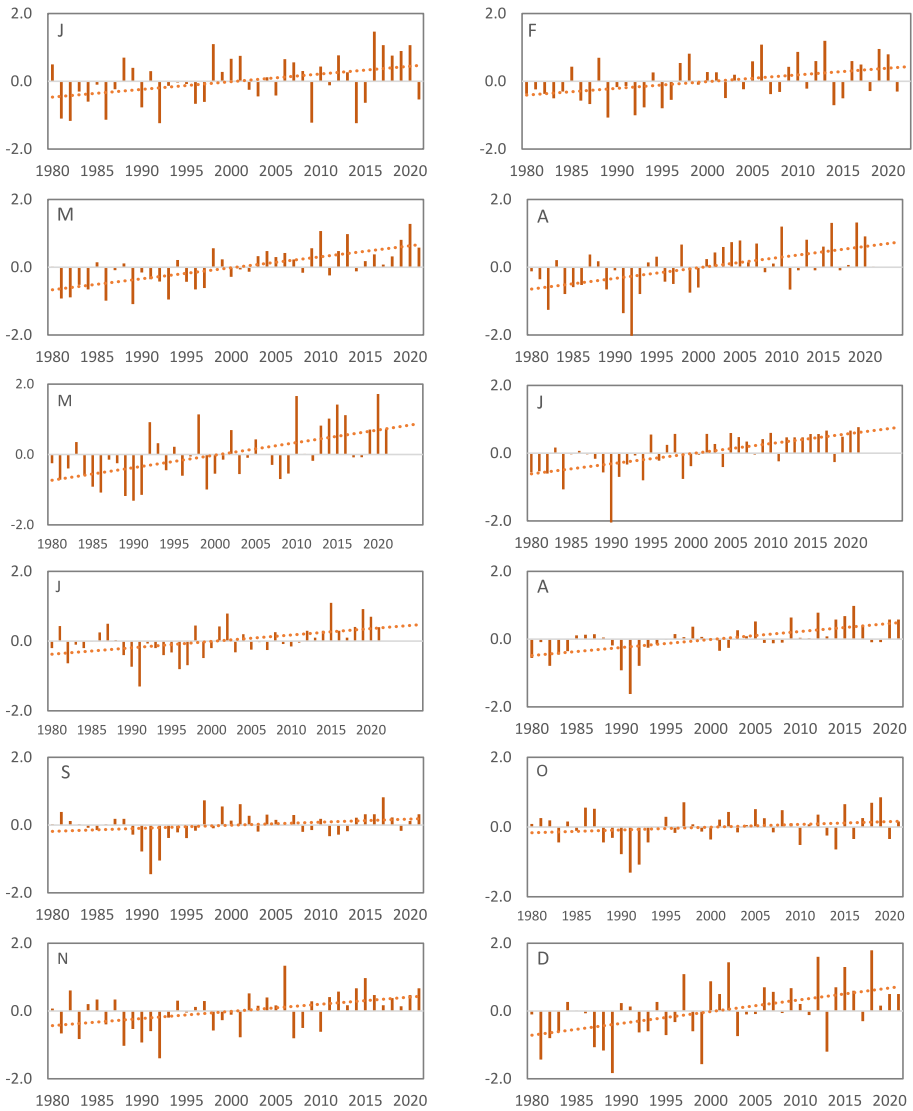
Fig. 4 Monthly mean temperature variability anomaly (1980–2021) at Chau Doc station. J–D denotes Jan–Dec. The X–axis represents Temperature ($^{\circ}$C), and the Y–axis represents the yearly time

droughts were least frequent at 13, 18, 13, and 12 occurrences. Notably, mild droughts were more common in both short (3-month) and long (12-month) timescales, whereas moderate and extreme droughts were more prevalent in medium-term (6- and 9-month) periods. Despite a brief period of negative SPIs during 2015–2016, the dataset exhibited pronounced drought events, particularly in 2002, characterized by exceptional SPI peak values across all time scales. The extreme SPI values of -3.01, -3.66, -3.69, and -3.83 were recorded for the 3-, 6-, 9-, and 12-month, respectively. The longest consecutive
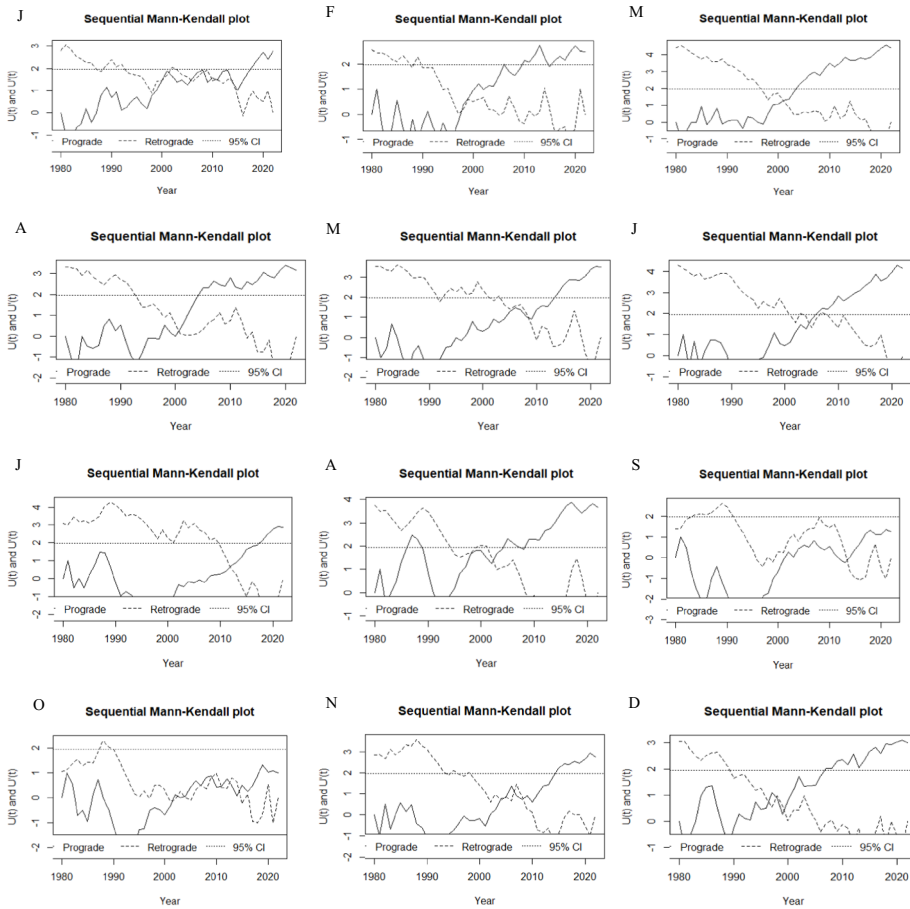
Fig. 5 Monthly average temperature trends using SMK plots at Chau Doc. J–D denotes Jan–Dec

drought period was eight months in 2002 for SPI 3, while SPI 6 and SPI 9 experienced two twelve-month drought events in 1992–1993 and 2002–2003. The most extended drought occurred for SPI 12 with a duration of 21 consecutive months in 2014–2016.

Similarly, the SPEI trend and SMK analysis for Chau Doc were calculated and the results are presented in Fig. 7. Mild drought events were the most prevalent, occurring 60, 47, 53, and 50 times for the 3-, 6-, 9-, and 12-month SPEI, respectively. Moderate drought events followed with frequencies of 26, 25, 29, and 37 occurrences, while extreme droughts were least frequent at 8, 12, 7, and 5 events across the corresponding time scales. Notably, mild droughts were more common in both short (3-month) and medium-term (9-month) timescales, whereas moderate drought was more prevalent in long-term (12-month) timescale, and extreme drought was more prevalent in medium-term (6-month) timescale. The SPEI was more sensitive to mild and moderate drought conditions than the SPI, however, the SPI was better at identifying extreme drought occurrences than the SPEI. The SMK test identified a non-significant, extended dry period based on SPEI values between 1985 and 1995. In contrast, the MK test found a statistically significant increase in SPEI levels between 1980 and 2021 while SPI did not show a clear temporal pattern the
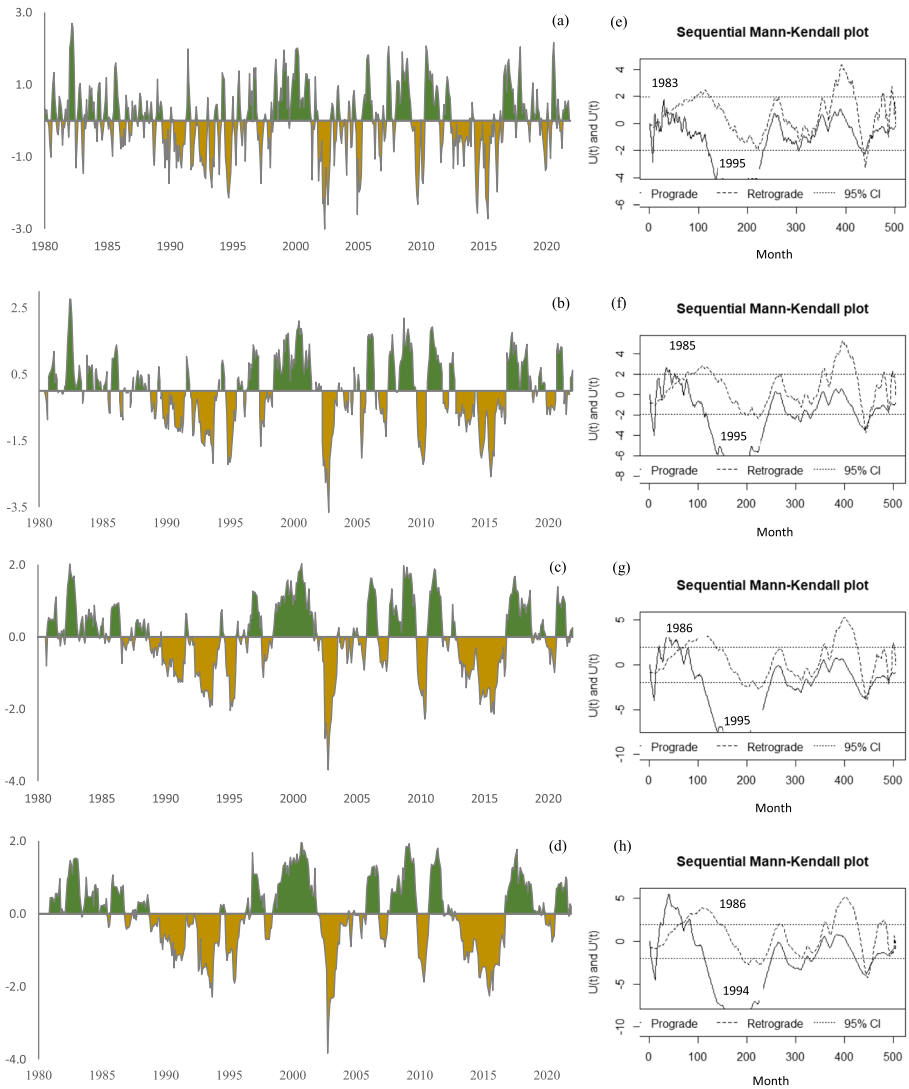
Fig. 6 Drought characteristics using SPI and SMK plots at time scales: SPI 3 (**a**), SPI 6 (**b**), SPI 9 (**c**), SPI 12 (**d**) and SMK 3 (**e**), SMK 6 (**f**), SMK 9 (**g**), SMK 12 (**h**). The X–axis represents SPI, and the Y–axis represents the yearly time (**a–d**)

same duration. The most extreme drought conditions occurred in 1983, with a SPI-3 value of -2.33. For the longer time scales, peak drought severity was observed in 1993, with SPI 6, SPI 9, and SPI 12 values of −2.12, −2.074, and −2.146, respectively. Analysis of drought duration revealed a maximum of eight consecutive dry months in 1992 for SPI 3, fifteen months for SPI 6 in 1992–1993, twenty-one months for SPI 9 in 1992–1994, and a prolonged twenty-four-month drought for SPI 12 in 1989–1991.
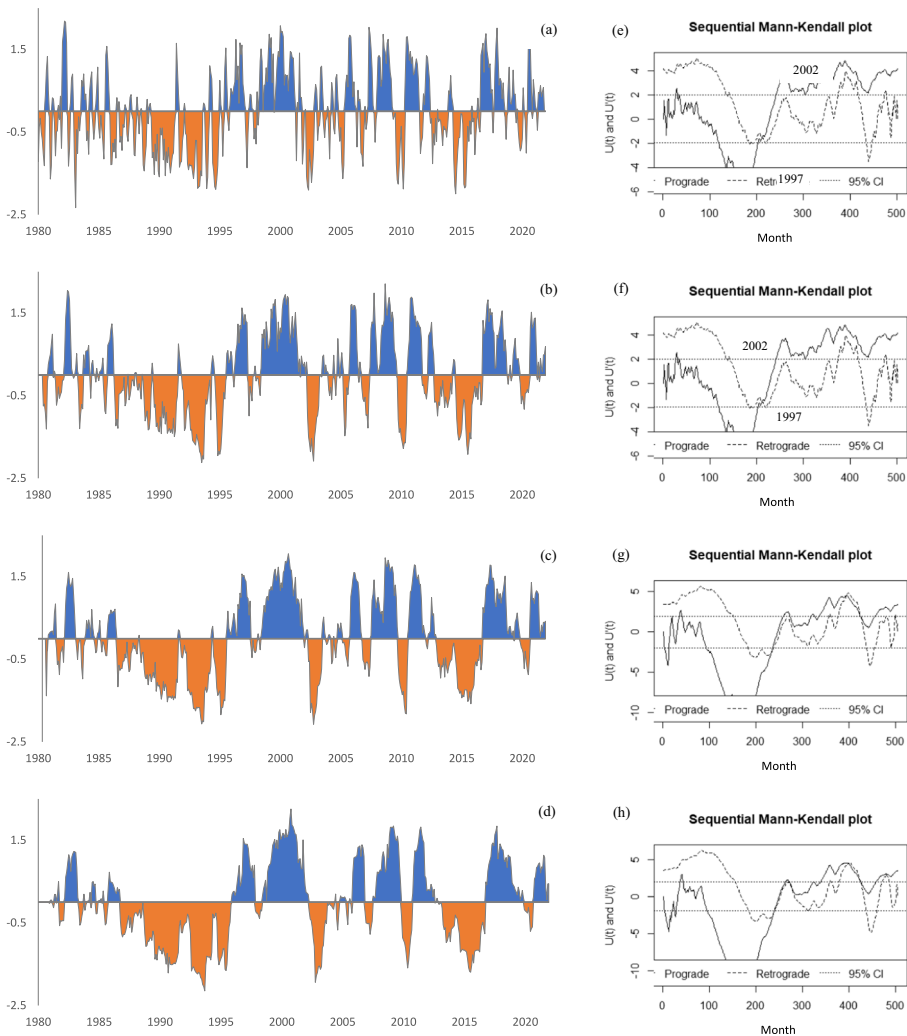
Fig. 7 Drought characteristics SPEI and SMK plots at time scales: SPEI 3 (**a**), SPEI 6 (**b**), SPEI 9 (**c**), SPEI 12 (**d**) and SMK 3 (**e**), SMK 6 (**f**), SMK 9 (**g**), SMK 12 (**h**). The X–axis represents SPEI, and the Y–axis represents the yearly time (**a**–**d**)

3.3 Hydrological regime changes

Accurate quantification of water availability, as a crucial element of the overall hydrological water balance, is essential for effective water resource assessment and management. The analysis revealed statistically significant declining trends in annual water levels at Tan Chau and Chau Doc, along with a decrease in annual river discharge at Chau Doc from 2000 to 2021 (Fig. 8). Specifically, the mean annual water level declined by -4.841 cm/year at Tan Chau and -3.433 cm/year at Chau Doc. Concurrently, Chau Doc experienced a mean annual discharge reduction of -43.212 m^3/s/year. The average annual reduction in water levels was -4.841 cm/year at Tan Chau and -3.433 cm/year at Chau Doc, while the

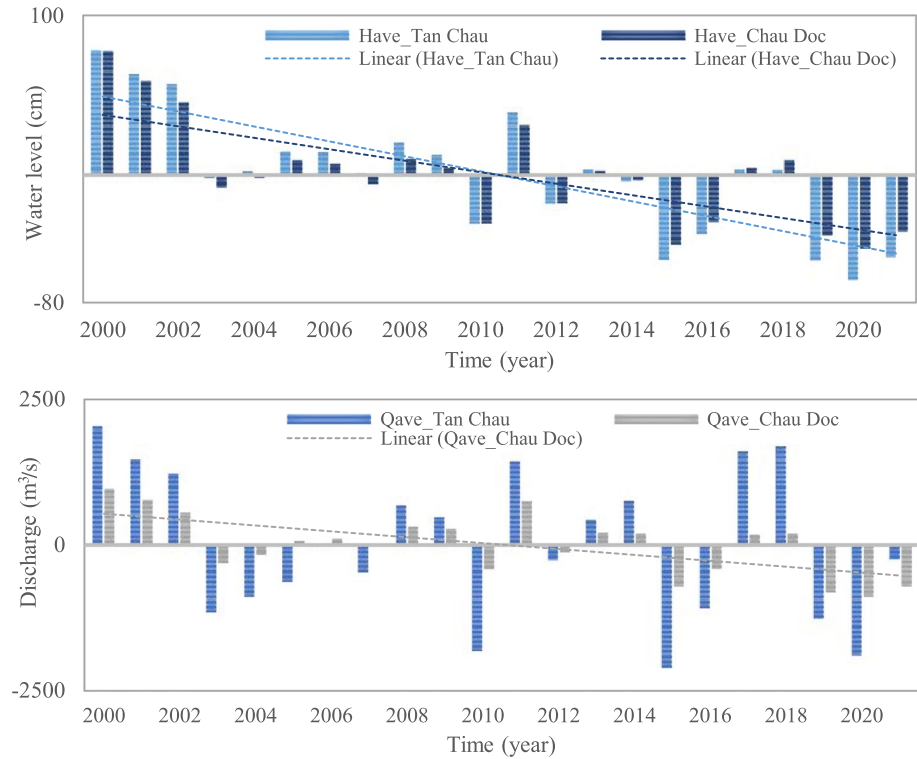**Fig. 8** Anomalies in annual water levels and discharges at Tan Chau and Chau Doc

average annual decline in discharge at Chau Doc was -43.212 m^3/s/year. During the dry season (July–Nov), water levels generally tended to decrease at both stations. At a 95% confidence level, significant drops in water levels were observed from Dec to Feb at Tan Chau, and during two specific months—Dec and Apr—at Chau Doc. The water levels rose between Mar and May; however, this increase was not statistically significant at the 5% level. Tan Chau and Chau Doc have distinct flow change trends. Except for Mar, May, and Jun, discharge at Chau Doc tended to drop at the 95% significance level, with only the discharge in Apr showing a statistically significant increasing trend at Tan Chau.

In general, the earliest decline in monthly water levels was recorded in Sept and Aug; nevertheless, the water levels began to decrease from 2006 to 2009, and this decrease became statistically significant after 2006 and 2009, respectively (Fig. 9). Both Oct and Nov water levels have been steadily decreasing since 2011, but becoming a statistically significant reduction since 2013 and 2014, respectively. Water levels in Jun and July fluctuated significantly more than those in other months over the years (CV = 0.407 and 0.434, respectively). Water levels in Jun-July have been steadily decreasing since 2011 and 2014 and have dropped significantly between 2009 and 2019. The water levels in the remaining months of the dry season were significantly lower between 2012 and 2020. Overall, annual water levels have been decreasing since 2011 and have significantly decreased since 2013. Fig. 12 demonstrates that the changes in water levels at Chau Doc were similar to those at Tan Chau. However, the time of water level drop starts at 1–2 months early (Table 2).
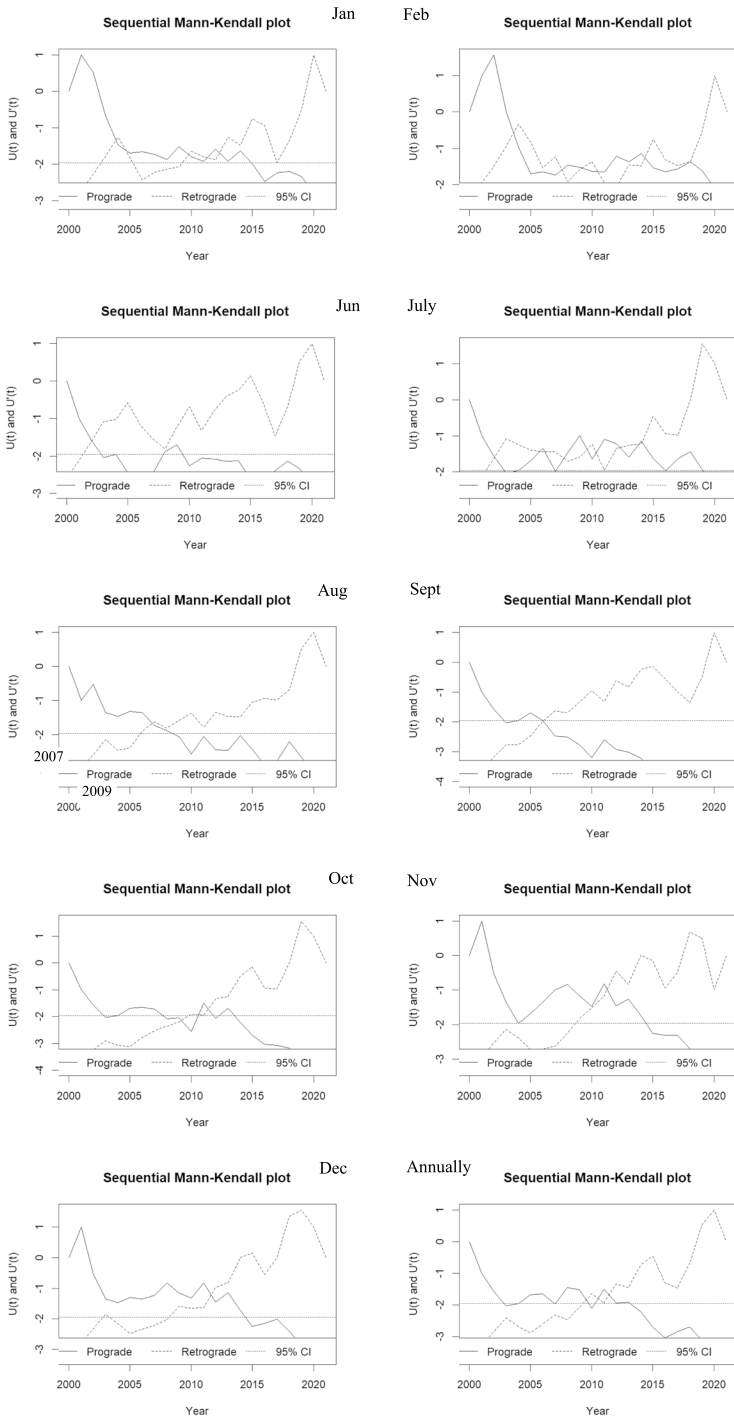
Fig. 9 SMK plots of monthly and annual water levels at Tan Chau (2000–2021). J-F denotes January–February, J–D denotes June–December

Table 2 Statistical analysis and Sen's slopes estimation

Variable	Have Tan Chau (cm)						Have Chau Doc (cm)					
	Mean	Std. deviation	CV	Kendall's tau	p-value	Sen's slope	Mean	Std. deviation	CV	Kendall's tau	p-value	Sen's slope
Jan	109.318	22.886	0.209	−0.469	0.003	−2.333	102.909	16.581	0.161	0.296	0.059	−1.000
Feb	81.045	13.940	0.172	−0.371	0.018	−1.375	79.727	10.530	0.132	−0.070	0.671	−0.133
Mar	63.500	9.898	0.156	−0.206	0.193	−0.526	64.955	9.297	0.143	0.192	0.225	0.500
Apr	52.909	6.782	0.128	0.225	0.157	0.333	54.682	10.073	0.184	0.510	0.001	1.167
May	53.318	13.629	0.256	−0.048	0.778	−0.200	52.864	12.468	0.236	0.261	0.096	0.667
Jun	85.000	34.626	0.407	−0.420	0.007	−3.500	74.727	24.873	0.333	−0.269	0.085	−1.824
July	155.364	67.492	0.434	−0.394	0.011	−5.818	127.318	52.293	0.411	−0.338	0.030	−3.846
Aug	265.727	88.006	0.331	−0.515	0.001	−10.000	217.727	75.853	0.348	−0.497	0.001	−8.750
Sept	327.909	91.916	0.280	−0.607	<0.0001	−12.750	283.864	90.549	0.319	−0.581	0.000	−11.824
Oct	332.364	82.450	0.248	−0.604	<0.0001	−10.500	299.318	77.617	0.259	−0.599	0.000	−10.333
Nov	238.500	66.511	0.279	−0.506	0.001	−7.450	218.364	58.324	0.267	−0.506	0.001	−6.071
Dec	154.727	39.290	0.254	−0.497	0.001	−4.214	142.773	31.171	0.218	−0.382	0.014	−3.000
Have	159.973	38.471	0.240	−0.564	0.000	−4.841	143.269	32.196	0.225	−0.489	0.002	−3.422

Variable	Qave Tan Chau (m³/s)						Qave Chau Doc (m³/s)					
	Mean	Std. deviation	CV	Kendall's tau	p-value	Sen's slope	Mean	Std. deviation	CV	Kendall's tau	p-value	Sen's slope
Jan	6225.000	1337.965	0.215	−0.174	0.271	−53.333	1181.304	395.673	0.335	−0.436	0.004	−39.412
Feb	4065.455	955.160	0.235	−0.182	0.247	−45.333	697.435	202.523	0.290	−0.344	0.023	−15.294
Mar	2968.182	763.810	0.257	0.126	0.430	25.556	491.652	123.998	0.252	−0.043	0.792	−1.333
Apr	2866.818	826.291	0.288	0.413	0.008	84.000	484.609	126.194	0.260	0.328	0.030	10.286
May	3812.727	1097.075	0.288	0.239	0.128	76.000	653.739	219.989	0.337	0.138	0.369	7.842
Jun	7368.636	2586.751	0.351	−0.186	0.236	−115.714	1305.000	520.443	0.399	−0.202	0.187	−26.471
July	12,293.636	3890.367	0.316	−0.174	0.271	−230.909	2495.348	1023.602	0.410	−0.328	0.030	−69.867
Aug	17,840.909	3007.239	0.169	−0.275	0.080	−246.667	4323.043	1307.365	0.302	−0.356	0.019	−110.476

Table 2 (continued)

Variable	Qave Tan Chau (m³/s)						Qave Chau Doc (m³/s)					
	Mean	Std. deviation	CV	Kendall's tau	p-value	Sen's slope	Mean	Std. deviation	CV	Kendall's tau	p-value	Sen's slope
Sept	19,709.091	2325.001	0.118	−0.238	0.128	−171.429	5346.522	1225.615	0.229	−0.478	0.002	−113.889
Oct	18,981.818	1778.077	0.094	−0.018	0.932	0.000	5334.348	1050.237	0.197	−0.436	0.004	−83.846
Nov	14,420.455	2483.144	0.172	0.009	0.977	7.143	3705.652	988.561	0.267	−0.317	0.037	−60.000
Dec	9774.091	2015.489	0.206	−0.121	0.446	−55.714	2078.870	638.316	0.307	−0.364	0.016	−50.000
Qave	10,027.235	1262.432	0.126	−0.152	0.338	−54.936	2341.460	507.636	0.217	−0.407	0.007	−43.212

Figure 10 shows the changes in discharge at Chau Doc using the SMK. The discharge changes at Tan Chau and Chau Doc are different. If only Apr displays a rise in the water level at Tan Chau, the other months and even the annual discharge show no trends. The decreasing discharge pattern at Chau Doc station was found to be similar to the water level at Chau Doc station, with the exception of increasing discharge in Apr.

Although mild–to–severe droughts have occurred in the study area, they have had an impact on the decrease in water levels and discharges. Although the SPI does not demonstrate an increase in dryness from 1980 to 2021, the SPEI shows that the study area is becoming wetter. However, in recent years, water levels and discharges have decreased despite the increase in rainfall, particularly during La Nina (2020–2021). The average temperature data revealed an increasing tendency, and the effects of hydroelectric dams will reduce the water budget because more than 60% of the water in the Mekong Delta originates from the upper sub-basins of the Mekong River Basin.

3.4 Drought characterizes assessment using run theory

The analysis identified 18 drought events based on the SPI, including nine single-month events, with a maximum drought duration of nine months (Fig. 11a). For the SSI at Chau Doc, 13 drought events were recorded, including one single-month event, and a longest duration of 18 months (Fig. 11b). At Tan Chau, the SSI indicated 10 drought events, with one single-month event and a maximum duration of 24 months (Fig. 11c). The average drought intensities for SPI, SSI at Chau Doc (SSI_CD), and SSI at Tan Chau (SSI_TC) were calculated as -0.882, -1.365, and -0.956, respectively. The most severe drought events recorded intensities of -1.972 for SPI, -1.940 for SSI_CD, and -2.243 for SSI_TC. Conversely, the least intense droughts exhibited values of -0.404, -1.065, and -0.67 for SPI, SSI_CD, and SSI_TC, respectively.

The research shows a high probability of concurrent meteorological and hydrological drought events at Chau Doc and Tan Chau stations, with 71% and 63% of hydrological droughts occurring in response to meteorological droughts, respectively. During the study period (2000–2021), a consistent time lag was observed between the occurrence of SPI and SSI at both Chau Doc and Tan Chau stations. The average time lag was four months at Chau Doc and two and a half months at Tan Chau. The earlier decade (2000–2010) had longer lag times (six months at Chau Doc and four months at Tan Chau), whereas the latter decade (2011–2021) had a significant reduction in lag, with an average lag of two months at Chau Doc and one month at Tan Chau. It should be noted that hydrological drought occurrences at Chau Doc and Tan Chau arrived before meteorological drought events in certain years between 2011 and 2021. This coincides with the operational period of the Mega hydropower dams on the Mekong River system.

4 Discussion

Located inland within the Mekong Delta, the study area experiences significantly lower average annual rainfall compared to the delta's overall average, primarily due to its greater distance from the sea (Minh et al. 2024b). While our findings revealed no statistically significant trend in annual rainfall, the increased temperature poses a significant risk to the region's water resource balance. The average temperature in the study area, which has risen steadily over the past
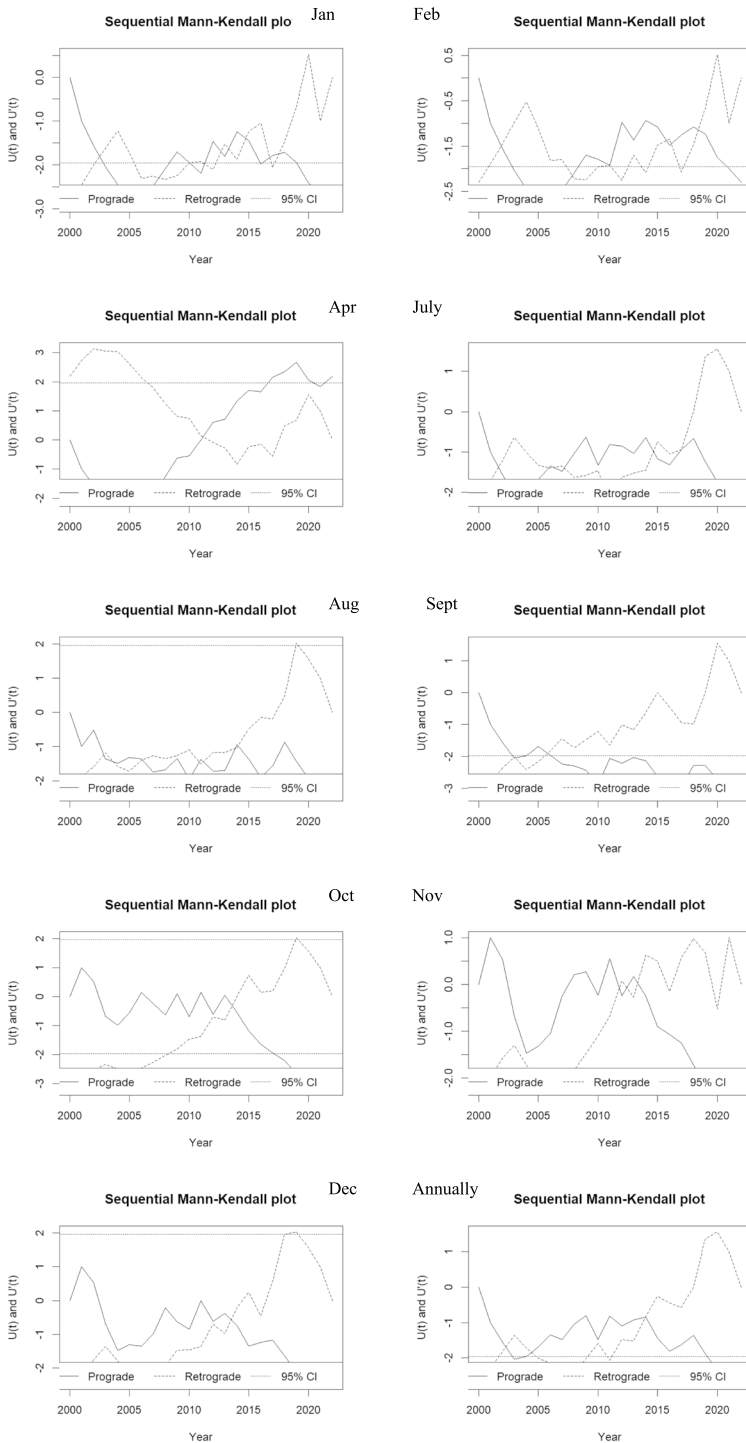
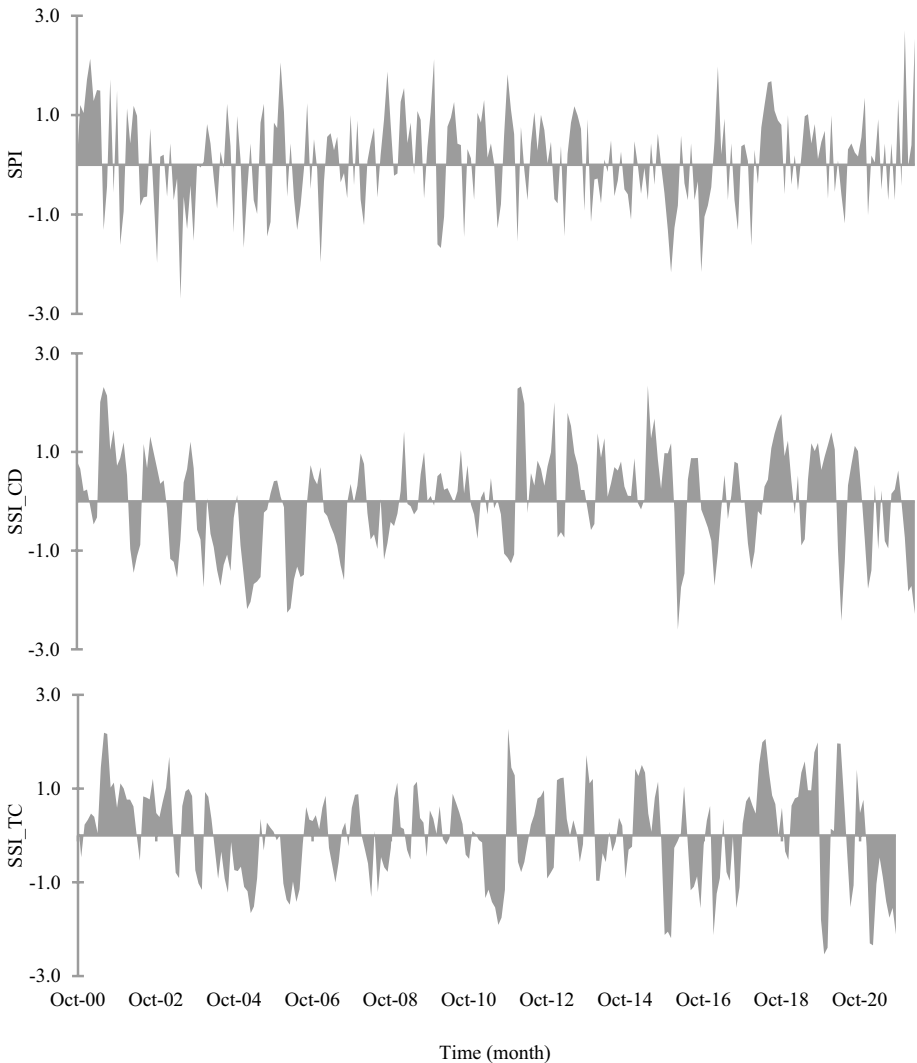**Fig. 10** SMK plots of monthly and annual discharge at Chau Doc (2000–2021). J–D denotes June–December

Fig. 11 Drought events identified using monthly SPI and SSI data for the period 2000 to 2021

decades, is particularly concerning because higher temperatures accelerate evapotranspiration rates, which, in turn, exacerbate water scarcity. The effects of this temperature rise are amplified by the reduction in water flow from the Mekong River system, which contributes to an increasingly fragile hydrological balance. These findings align with existing studies that have documented similar warming trends across Southeast Asia (Van Binh et al. 2020; Li et al. 2023).

In line with existing literature, such as Van Binh et al. (2020), our study confirms that human activities, particularly upstream hydroelectric operations, have had a more substantial impact on water flows in the lower Mekong River basin than climate change. This influence is especially noticeable in the dry season, where the increasing demand for water for irrigation has compounded the region's water scarcity. Despite an observed decrease in flood flow, our results align with numerous studies (Li et al. 2023; Tang et al. 2023),

that indicate increased variability in dry season flows. Our analysis found that while some months during the wet season experienced above-average rainfall, the dry season saw increased rainfall variability, particularly in typically drier months like January and February. This aligns with findings by Keovilignavong et al. (2023), who also emphasize the influence of human interventions on drought conditions in the Mekong region.

Furthermore, (Li et al. 2023) highlighted a probable reduction in flood risks but a strong increase in drought risks in Mekong River Basin countries, including Vietnam. This aligns with our findings, as we observed increased risks of drought in the study area, particularly due to the decreased upstream flow and the lowering of the major river water levels in the VMD. This reduction in upstream flow, combined with the operation of salinity gates designed to restrict saltwater intrusion into the canals, has created a more precarious water management situation. Saltwater intrusion into the main rivers of the VMD, exacerbated by these hydrological changes, poses a significant threat to agriculture and freshwater availability in the region (Van Binh et al. 2020; Park et al. 2022).

Our analysis of discharge fluctuations at Tan Chau and Chau Doc stations provides further evidence of the influence of both natural and human-induced factors on the region's hydrology. El Niño events have historically resulted in lower discharges, a pattern that was observed in our study during the El Niño periods of 2002, 2004–2006, 2009–2010, 2014–2015, and 2018–2019. Despite the wetter conditions typically associated with La Niña events, the decline in discharge persisted during recent La Niña years (2020–2021). This suggests that upstream water management, including dam operations, may be overriding the effects of natural climatic variability. Recent research supports this assertion, indicating that hydropower dams in the upper Mekong River basin have exacerbated hydrological drought conditions in the lower Mekong region (Lu and Chua 2021; Phung et al. 2021; Keovilignavong et al. 2023). This is consistent with broader research on ENSO's impacts on river basins globally, as similar patterns have been observed in other regions, such as the Blue Nile River Basin (Abtew et al. 2009).

Furthermore, the Mann–Kendall and Sen's slope tests revealed significant upward trends in temperature across the region, with an average increase of 0.26 °C per decade. May experienced the most rapid temperature rise, with a slope of 0.34 °C per decade, while December showed the slowest rate at 0.18 °C per decade. These increasing temperatures, particularly during the dry season, compound the challenges of water scarcity and place additional stress on the region's agricultural systems.

Our drought analysis using SPI and SPEI further highlights the complexity of the region's hydrology. Mild drought events were the most prevalent across all timescales, while extreme droughts were less frequent but more severe when they occurred. Interestingly, the SPEI appeared to be more sensitive to identifying mild and moderate drought conditions, whereas the SPI was more effective in detecting extreme drought occurrences. These findings are consistent with other studies that have explored drought indices and their sensitivity, such as the work by Beguería et al. (2014) on the SPEI. The SPEI analysis indicated an extended dry period from 1985 to 1995, though the more recent period from 1980 to 2021 showed statistically significant increases in SPEI levels, suggesting an overall trend toward wetter conditions. However, the SPI did not display a clear temporal pattern, indicating the presence of complex, multifaceted changes in the region's hydrological cycle.

A notable finding from our study is the shifting temporal relationship between meteorological and hydrological droughts. During the 2000–2010 period, meteorological droughts typically preceded hydrological droughts by 4–6 months. However, in the 2011–2021 period, this lag shortened to 1–2 months, and in some cases, hydrological droughts even

preceded meteorological droughts. This shift could be attributed to the cumulative impact of upstream water management and hydropower development, which have altered the timing and intensity of water flows in the lower Mekong. The shortening of this lag time highlights the need for more adaptive and flexible water management strategies to address the increasingly rapid and unpredictable changes in the region's hydrology. This finding aligns with the work of Gan et al. (2024) and other researchers who have analyzed hydrological drought propagation and the impacts of human modifications on river systems.

These findings highlight the critical need for integrated water management strategies that consider both natural climatic variability and the substantial impacts of human activities. The combined effects of rising temperatures, increased drought risks, and hydropower development in the upper Mekong basin have fundamentally altered the hydrological balance of the Mekong Delta (Van Binh et al. 2020; Keovilignavong et al. 2023). Policymakers and water managers must adopt more flexible and responsive strategies to mitigate these impacts and ensure the sustainability of water resources and the livelihoods that depend on them (Lu and Chua 2021). Future research needs to focus on the long-term impacts of upstream hydropower development and climate change on the Mekong Delta, with a particular emphasis on mitigating the increasing risks of drought and saltwater intrusion (Park et al. 2022; Minh et al. 2024a).

5 Conclusions

While rainfall in the study area showed no statistically significant trend, temperature increases were significant, with the dry season experiencing earlier temperature rises than the wet season. The average monthly temperature during the dry season began increasing around the year 2000, while the average monthly temperature during the rainy season increased between 2005 and 2019. Compared to the rest of the year, December, March, and May tended to have the highest increases. Both the SPI and SPEI indices identified the temporal variability of droughts and were able to identify different types of droughts, as indicated by the different timescales. It was found that SPIs can respond better to extreme drought events than SPEIs, while SPEIs can detect El Niño year events in this region. The annual water levels in three months (Sep-Nov) decreased from 2010 to 2013, with a significant drop beginning in 2013 in Tan Chau. Similarly, for Chau Doc, the annual water levels in Sept-Nov began to decrease around 2013 and became statistically significant in 2019, 2019, and 2015. The annual discharge at the Tan Chau station showed no significant trend, whereas the mean annual discharge at Chau Doc showed a decreasing trend that began around 2001 and became significant around 2003. Although there is no clear trend in rainfall, the average temperature has increased, resulting in drier conditions. At that time, the demand for water for crops and daily life will increase because of increased evaporation. Furthermore, in recent years, flow in the Mekong Delta has decreased significantly during the wet season.
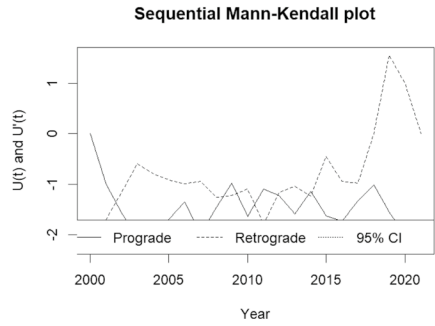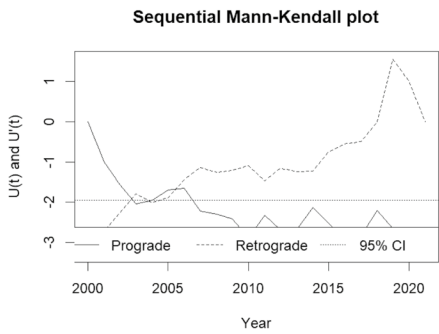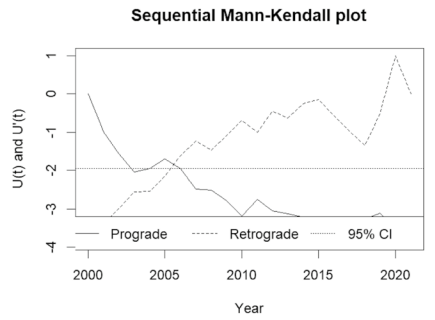
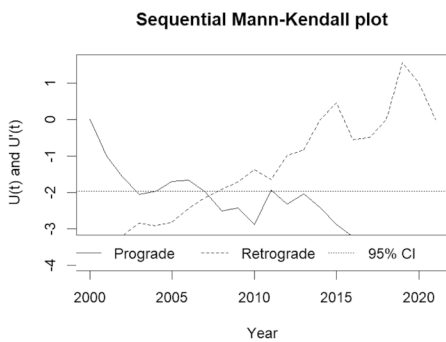## Appendix A

See Fig. 12.

Apr
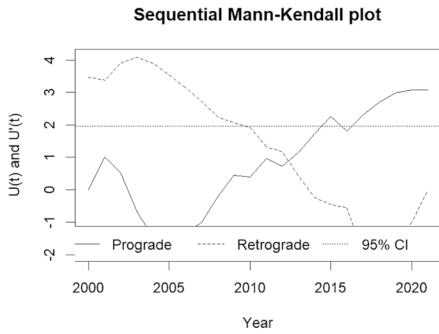
July

Aug

Sept

Oct

Nov

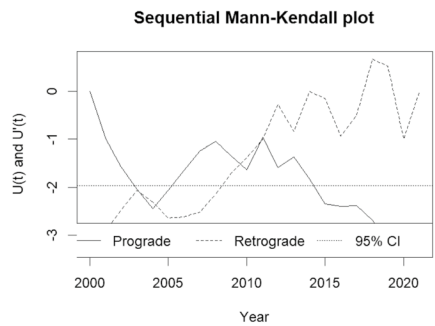**Fig. 12** SMK plots of monthly and annually water levels at Chau Doc (2000–2021). From J-D denotes June–December

Dec   **Annually**
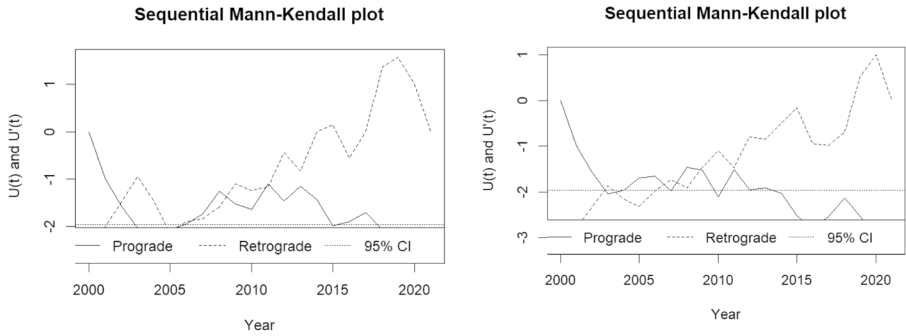

Fig. 12 (continued)

Appendix B

See Table 3.

Table 3 Mann–Kendall test and Sen's slope results for average monthly temperature at Chau Doc

Months	Z	S	Vars	Tau	Sen's slope	P-value
Jan	2.17	224	8512	0.26	0.027	0.0156
Feb	2.53	234	8510	0,27	0.022	0.0122
Mar	4.56	425	8513	0.49	0.033	0.0000
Apr	3.35	310	8504	0.36	0.029	0.001
May	3.52	326	8513	0.38	0.034	0.000
Jun	4.36	403	8505	0.47	0.027	0.000
July	3.03	280	8500	0.33	0.018	0.002
Aug	3.86	357	8508	0.42	0.023	0.000
Sept	1.43	133	8504	0.16	0.006	0.152
Oct	1.10	102	8505	0.12	0.007	0.274
Nov	2.97	275	8510	0.32	0.021	0.003
Dec	3.12	289	8504	0.34	0.033	0.002

Declarations

Conflicts of interest The authors declare no conflicts of interest.

Ethical approval Not applicable.

Consent to participate Agree to participate.

Consent to publish Agree to publish.

References

Abbasi A, Khalili K, Behmanesh J, Shirzad A (2019) Drought monitoring and prediction using SPEI index and gene expression programming model in the west of Urmia Lake. Theoret Appl Climatol 138:553–567

Abtew W, Melesse AM, Dessalegne T (2009) El Niño southern oscillation link to the Blue Nile River basin hydrology. Hydrol Process Int J 23:3653–3660

Amatya B, Khan F (2023) Climate change and disability: a physical medicine and rehabilitation (PM&R) perspective. J Int Soc Phys Rehabil Med 6:5–9

Beguería S, Vicente-Serrano SM, Reig F, Latorre B (2014) Standardized precipitation evapotranspiration index (SPEI) revisited: parameter fitting, evapotranspiration models, tools, datasets and drought monitoring. Int J Climatol 34:3001–3023

Bihrat Ö, Bayazit M (2003) The power of statistical tests for trend detection. Turk J Eng Environ Sci 27:247–251

Binh DV, Kantoush S, Sumi T et al (2017) Study on the impacts of river-damming and climate change on the Mekong Delta of Vietnam. 京都大学防災研究所年報B 60:804–826

Boroneant C, Ionita M, Brunet M, Rimbu N (2011) CLIVAR-SPAIN contributions: Seasonal drought variability over the Iberian Peninsula and its relationship to global sea surface temperature and large scale atmospheric circulation. WCRP OSC: Climate Research in Service to Society pp 24–28

Cancelliere A, Salas JD (2004) Drought length properties for periodic-stochastic hydrologic data. Water Resour Res 40:13

Chandimala J, Zubair L (2007) Predictability of stream flow and rainfall based on ENSO for water resources management in Sri Lanka. J Hydrol 335:303–312

Chiew FHS, McMahon TA (2002) Global ENSO-streamflow teleconnection, streamflow forecasting and interannual variability. Hydrol Sci J 47:505–522. https://doi.org/10.1080/02626660209492950

Danandeh Mehr A, Vaheddoost B (2020) Identification of the trends associated with the SPI and SPEI indices across Ankara, Turkey. Theoret Appl Climatol 139:1531–1542

Darby SE, Leyland J, Kummu M et al (2013) Decoding the drivers of bank erosion on the Mekong river: the roles of the Asian monsoon, tropical storms, and snowmelt. Water Resour Res 49:2146–2163

Dat TV (2020) Proposing a research framework to improve institutions and policies to reduce risks of flash floods and landslides. Vietnam J OnLine 8(10):e10701

Diaz HF, Diaz HF, Markgraf V, Diaz HF (1992) El Niño: historical and paleoclimatic aspects of the Southern Oscillation. Cambridge University Press, Cambridge

Esteban-Parra M, Rodrigo F, Castro-Diez Y (1995) Temperature trends and change points in the Northern Spanish Plateau during the last 100 years. Int J Climatol 15:1031–1042

Food and Agriculture Organization (FAO). (2016) El Niñoevent in Vietnam: Agriculture, food security andlivelihood need assessment in response to drought andsalt water intrusion. Ha Noi, Vietnam

Fuchs B (2012) "A new national drought risk Atlas for the US from the National Drought Mitigation Center." National Drought Mitigation Center, University of Nebraska, Lincoln, NE, USA

Gan R, Gu S, Tong X et al (2024) A nonparametric standardized runoff index for characterizing hydrological drought in the Shaying River Basin, China. Nat Hazards 120:2233–2253

General Statistics Office Of Vietnam (GSO). (2020) Statistical year book of Vietnam 2020. General Statistics Office of Vietnam, Ha Noi, Vietnam

Gumus V, Simsek O, Avsaroglu Y, Agun B (2021) Spatio-temporal trend analysis of drought in the GAP Region, Turkey. Nat Hazards 109:1759–1776

Hao Z, Singh VP (2015) Drought characterization from a multivariate perspective: a review. J Hydrol 527:668–678

Heim RR Jr (2002) A review of twentieth-century drought indices used in the United States. Bull Am Meteor Soc 83:1149–1166

Hirsch RM, Slack JR (1984) A nonparametric trend test for seasonal data with serial dependence. Water Resour Res 20:727–732

Hirsch RM, Helsel DR, Cohn TA, Gilroy EJ (1992) Statistical analysis of hydrologic data. Handb Hydrol 17:17–55

Hosking JR (1990) L-moments: Analysis and estimation of distributions using linear combinations of order statistics. J Roy Stat Soc: Ser B (Methodol) 52:105–124

Ji L, Peters AJ (2003) Assessing vegetation response to drought in the northern Great Plains using vegetation and drought indices. Remote Sens Environ 87:85–98

Kang H, Sridhar V (2024) Droughts in the Mekong Basin—Current situation and future prospects. The Mekong River Basin. Elsevier, Amsterdam, pp 115–154. https://doi.org/10.1016/B978-0-323-90814-6.00019-X

Keovilignavong O, Nguyen TH, Hirsch P (2023) Reviewing the causes of Mekong drought before and during 2019–20. Int J Water Resour Dev 39:155–175

Khan S, Gabriel H, Rana T (2008) Standard precipitation index to track drought and assess impact of rainfall on watertables in irrigation areas. Irrig Drain Syst 22:159–177

Kimmany B, Visessri S, Pech P, Ekkawatpanit C (2024) The impact of climate change on hydro-meteorological droughts in the Chao Phraya River Basin. Water, Thailand. https://doi.org/10.3390/w16071023

Krall J, Huba J, Fritts D (2013) On the seeding of equatorial spread F by gravity waves. Geophys Res Lett 40:661–664

Lam HC, Haines A, McGregor G et al (2019) Time-series study of associations between rates of people affected by disasters and the El Niño Southern Oscillation (ENSO) cycle. Int J Environ Res Public Health. https://doi.org/10.3390/ijerph16173146

Lavane K, Kumar P, Meraj G et al (2023) Assessing the effects of drought on rice yields in the Mekong Delta. Climate. https://doi.org/10.3390/cli11010013

Lee SK, Dang TA (2019) Spatio-temporal variations in meteorology drought over the Mekong River Delta of Vietnam in the recent decades. Paddy Water Environ 17:35–44. https://doi.org/10.1007/s10333-018-0681-8

Li X, Hui J, Sarah G et al (2017) Spatiotemporal variation of drought characteristics in the Huang-Huai-Hai Plain, China under the climate change scenario. J Integr Agric 16:2308–2322

Li Q, Zeng T, Chen Q et al (2023) Spatio-temporal changes in daily extreme precipitation for the Lancang-Mekong River Basin. Nat Hazards 115:641–672

Li Y, Feng Y, Zhang B, Zhang C (2024a) Drought propagation across meteorological, hydrological and agricultural systems in the Lancang-Mekong River Basin. Hydrol Process 38:e15130

Li Y, Yuan F, Zhou Q, Liu F, Biswas A, Yang G, Liao Z (2024b) Spatial and temporal variations of SPI and SSI. In: Li Y, Yuan F, Zhou Q, Liu F, Biswas A, Yang G, Liao Z (eds) Spatiotemporal Dynamics of Meteorological and Agricultural Drought in China. Springer, Singapore, pp 43–58. https://doi.org/10.1007/978-981-97-4214-1_3

Lu XX, Chua SDX (2021) River discharge and water level changes in the Mekong River: droughts in an era of mega-dams. Hydrol Process 35:e14265

Ma Q, Li F, Liu F et al (2023) SPEI and multi-threshold run theory based drought analysis using multi-source products in China. J Hydrol 616:128737

Mann HB (1945) Nonparametric tests against trend. Econometrica 13(3):245. https://doi.org/10.2307/1907187

McKee, Thomas B., Nolan J. Doesken, and John Kleist. "The relationship of drought frequency and duration to time scales." In: Proceedings of the 8th Conference on Applied Climatology. Vol. 17. No. 22. 1993

Mesbahzadeh T, Mirakbari M, Mohseni Saravi M et al (2020) Meteorological drought analysis using copula theory and drought indicators under climate change scenarios (RCP). Meteorol Appl 27:e1856

Minh HVT, Kumar P, Van Ty T et al (2022a) Understanding dry and wet conditions in the Vietnamese Mekong Delta using multiple drought indices: a case study in Ca Mau Province. Hydrology 9:213

Minh HVT, Van Ty T, Avtar R et al (2022b) Implications of climate change and drought on water requirements in a semi-mountainous region of the Vietnamese Mekong Delta. Environ Monit Assess 194:1–20

Minh HVT, Kumar P, Van Toan N et al (2024a) Deciphering the relationship between meteorological and hydrological drought in Ben Tre province, Vietnam. Nat Hazards. https://doi.org/10.1007/s11069-024-06437-z

Minh HVT, Lien BTB, Hong Ngoc DT et al (2024b) Understanding rainfall distribution characteristics over the Vietnamese Mekong Delta: a comparison between coastal and inland localities. Atmosphere 15:217

Minh HVT, Van Ty T, Nam NDG et al (2024c) Modelling and predicting annual rainfall over the Vietnamese Mekong Delta (VMD) using SARIMA. Discov Geosci 2:19

Mishra AK, Singh VP (2010) A review of drought concepts. J Hydrol 391:202–216

Mitra S, Srivastava P (2017) Spatiotemporal variability of meteorological droughts in southeastern USA. Nat Hazards 86:1007–1038

Moyé LA, Kapadia AS, Cech IM, Hardy RJ (1988) The theory of runs with applications to drought prediction. J Hydrol 103:127–137

Naderi K, Moghaddasi M, Shokri A (2022) Drought occurrence probability analysis using multivariate standardized drought index and copula function under climate change. Water Resour Manag 36:2865–2888

Nalbantis I, Tsakiris G (2009) Assessment of hydrological drought revisited. Water Resour Manag 23:881–897

Nalley D, Adamowski J, Khalil B, Ozga-Zielinski B (2013) Trend detection in surface air temperature in Ontario and Quebec, Canada during 1967–2006 using the discrete wavelet transform. Atmos Res 132:375–398

Nguyen T-T-H, Li M-H, Vu TM, Chen P-Y (2023) Multiple drought indices and their teleconnections with ENSO in various spatiotemporal scales over the Mekong River Basin. Sci Total Environ 854:158589. https://doi.org/10.1016/j.scitotenv.2022.158589

Ogunbode CA, Doran R, Böhm G (2020) Exposure to the IPCC special report on 1.5 °C global warming is linked to perceived threat and increased concern about climate change. Clim Change 158:361–375. https://doi.org/10.1007/s10584-019-02609-0

Panu U, Sharma T (2002) Challenges in drought research: some perspectives and future directions. Hydrol Sci J 47:S19–S30

Park E, Loc HH, Van Binh D, Kantoush S (2022) The worst 2020 saline water intrusion disaster of the past century in the Mekong Delta: impacts, causes, and management implications. Ambio 51:691–699

Partal T, Kahya E (2006) Trend analysis in Turkish precipitation data. Hydrol Process Int J 20:2011–2026

Paulo A, Rosa R, Pereira L (2012) Climate trends and behaviour of drought indices based on precipitation and evapotranspiration in Portugal. Nat Hazard 12:1481–1491

Phung D, Nguyen-Huy T, Tran NN et al (2021) Hydropower dams, river drought and health effects: a detection and attribution study in the lower Mekong Delta Region. Clim Risk Manag 32:100280

Polong F, Chen H, Sun S, Ongoma V (2019) Temporal and spatial evolution of the standard precipitation evapotranspiration index (SPEI) in the Tana River Basin, Kenya. Theoret Appl Climatol 138:777–792

Potop V, Možný M, Soukup J (2012) Drought evolution at various time scales in the lowland regions and their impact on vegetable crops in the Czech Republic. Agric for Meteorol 156:121–133

Quang C, Hoa H, Giang N, Hoa N (2021) Assessment of meteorological drought in the Vietnamese Mekong delta in period 1985–2018. IOP Publishing, Bristol, p 012020

Räsänen TA, Kummu M (2013) Spatiotemporal influences of ENSO on precipitation and flood pulse in the Mekong River Basin. J Hydrol 476:154–168

Roeckner E, Oberhuber J-M, Bacher A et al (1996) ENSO variability and atmospheric response in a global coupled atmosphere-ocean GCM. Clim Dyn 12:737–754

Ropelewski CF, Halpert MS (1986) North American precipitation and temperature patterns associated with the El Niño/Southern Oscillation (ENSO). Mon Weather Rev 114(12):2352–2362

Sattar MN, Lee J-Y, Shin J-Y, Kim T-W (2019) Probabilistic characteristics of drought propagation from meteorological to hydrological drought in South Korea. Water Resour Manag 33:2439–2452

Sen PK (1968) Estimates of the regression coefficient based on Kendall's tau. J Am Stat Assoc 63:1379–1389

Şen Z (1989) The theory of runs with applications to drought prediction—comment. J Hydrol 110:383–390

Shamshirband S, Hashemi S, Salimi H et al (2020) Predicting standardized streamflow index for hydrological drought using machine learning models. Eng App Comput Fluid Mech 14:339–350

Shehu A, Yelwa S, Sawa B, Adegbehin A (2016) The Influence of El-Niño Southern Oscillation (ENSO) phenomenon on rainfall variation in Kaduna Metropolis, Nigeria. J Geogr Environ Earth Sci Int 8:1–9

Sims AP, Dutta SND, Raman S (2002) Adopting drought indices for estimating soil moisture: a North Carolina case study. Geophys Res Lett 29:24–31

Singh U, Agarwal P, Sharma PK (2022) Meteorological drought analysis with different indices for the Betwa River basin, India. Theoret Appl Climatol 148:1741–1754. https://doi.org/10.1007/s00704-022-04027-2

Smith TM, Ropelewski CF (1997) Quantifying Southern Oscillation–precipitation relationships from an atmospheric GCM. J Clim 10:2277–2284

Sneyers R (1991) On the statistical analysis of series of observations, 143: 192

Sohn S, Ahn J, Tam C (2013) Six month–lead downscaling prediction of winter to spring drought in South Korea based on a multimodel ensemble. Geophys Res Lett 40:579–583

Szalai S, Szinell C, Zoboki J (2000) Drought monitoring in Hungary. Early Warn Syst Drought Prep Drought Manag 57:182–199

Tallaksen LM, Van Lanen HLJ (2004) Drought as a natural hazard. Hydrological drought processes and estimation methods for stream flow and groundwater. Elsevier, Amsterdam

Tang R, Dai Z, Mei X et al (2023) Secular trend in water discharge transport in the lower Mekong River-delta: Effects of multiple anthropogenic stressors, rainfall, and tropical cyclones. Estuar Coast Shelf Sci 281:108217

Tirivarombo S, Osupile D, Eliasson P (2018) Drought monitoring and analysis: standardised precipitation evapotranspiration index (SPEI) and standardised precipitation index (SPI). Phys Chem Earth, Parts a/b/c 106:1–10

Tran QD, Nguyen PT, Trinh TL et al (2022) Investigation of drought characteristics across Vietnam during period 1980–2018 using SPI and SPEI drought indices. VNU J Sci Earth Environ Sci 38:2588

Tri VPD, Yarina L, Nguyen HQ, Downes NK (2023) Progress toward resilient and sustainable water management in the Vietnamese Mekong Delta. Wiley Interdiscip Rev Water 10:e1670

Van Loon A, Laaha G (2015) Hydrological drought severity explained by climate and catchment characteristics. J Hydrol 526:3–14

Van Loon AF, Van Lanen HAJ (2013) Making the distinction between water scarcity and drought using an observation-modeling framework. Water Resour Res 49:1483–1502. https://doi.org/10.1002/wrcr.20147

Van Binh D, Kantoush SA, Saber M et al (2020) Long-term alterations of flow regimes of the Mekong River and adaptation strategies for the Vietnamese Mekong Delta. J Hydrol Regional Stud 32:100742

Van Loon AF, Stahl K, Di Baldassarre G et al (2016) Drought in a human-modified world: reframing drought definitions, understanding, and analysis approaches. Hydrol Earth Syst Sci 20:3631–3650

Vicente-Serrano SM (2006) Differences in spatial patterns of drought on different time scales: an analysis of the Iberian Peninsula. Water Resour Manage 20:37–60

Vicente-Serrano SM, Beguería S, López-Moreno JI (2010) A multiscalar drought index sensitive to global warming: the standardized precipitation evapotranspiration index. J Clim 23:1696–1718

Vicente-Serrano SM, López-Moreno JI, Gimeno L et al (2011) A multiscalar global evaluation of the impact of ENSO on droughts. J Geophy Res Atmos. https://doi.org/10.1029/2011JD016039

Wang W, Zhu Y, Xu R, Liu J (2015) Drought severity change in China during 1961–2012 indicated by SPI and SPEI. Nat Hazards 75:2437–2451

Wu J, Liu Z, Yao H et al (2018) Impacts of reservoir operations on multi-scale correlations between hydrological drought and meteorological drought. J Hydrol 563:726–736. https://doi.org/10.1016/j.jhydrol.2018.06.053

Wu R, Zhang J, Bao Y, Guo E (2019) Run theory and copula-based drought risk analysis for Songnen Grassland in Northeastern China. Sustainability. https://doi.org/10.3390/su11216032

Wu J, Chen X, Yao H, Zhang D (2021) Multi-timescale assessment of propagation thresholds from meteorological to hydrological drought. Sci Total Environ 765:144232

Xu Z, Takeuchi K, Ishidaira H (2003) Monotonic trend and step changes in Japanese precipitation. J Hydrol 279:144–150

Yevjevich VM (1967) An objective approach to definitions and investigations of continental hydrologic droughts. Vol. 23. Fort Collins, CO, USA: Colorado State University

Yusuf AA, Francisco H (2009) Climate change vulnerability mapping for Southeast Asia

Zalokar L, Kobold M, Šraj M (2021) Investigation of spatial and temporal variability of hydrological drought in Slovenia using the standardised streamflow index (SSI). Water. https://doi.org/10.3390/w13223197

Zeppel MJ, Macinnis-Ng CM, Yunusa IA et al (2008) Long term trends of stand transpiration in a remnant forest during wet and dry years. J Hydrol 349:200–213

Zhong F, Cheng Q, Wang P (2020) Meteorological drought, hydrological drought, and NDVI in the Heihe River basin, Northwest China: evolution and propagation. Adv Meteorol 2020:2409068

Authors and Affiliations

H. V. T. Minh[1] · **P. Kumar[2]** · **N. K. Downes[1]** · **N. V. Toan[3]** · **G. Meraj[4]** · **P. C. Nguyen[5]** · **K. N. Le[6]** · **T. V. Ty[7]** · **K. Lavane[8]** · **R. Avtar[9,10]** · **M. Almazroui[11]**

✉ P. Kumar
  kumar@iges.or.jp

  H. V. T. Minh
  hvtminh@ctu.edu.vn

  N. K. Downes
  nkdownes@ctu.edu.vn

  N. V. Toan
  nvtoan@ctu.edu.vn

  G. Meraj
  gowharmeraj@g.ecc.u-tokyo.ac.jp

  P. C. Nguyen
  pcnguyen@ctu.edu.vn

  K. N. Le
  lnkieu@ctu.edu.vn

  T. V. Ty
  tvty@ctu.edu.vn

  K. Lavane
  klavane@ctu.edu.vn

  R. Avtar
  ram@ees.hokudai.ac.jp

  M. Almazroui
  mansour@kau.edu.sa

[1] Water Resources Department, College of Environment and Natural Resources, Can Tho University, Can Tho City 900000, Vietnam

[2] Institute for Global Environmental Strategies, Hayama 240-0115, Japan

[3] Department of Personnel, Can Tho University, Can Tho City 900000, Vietnam

[4] Department of Ecosystem Studies, Graduate School of Agricultural and Life Sciences, The University of Tokyo, Tokyo 113-8654, Japan

[5] Department of Land Resources, Can Tho University, Can Tho City 900000, Vietnam

[6] Department of Environment and Natural Resources, Can Tho University, Can Tho City 900000, Vietnam

[7] Department of Water Resources Engineering, College of Technology, Can Tho University, Can Tho City 900000, Vietnam

[8] Department of Environmental Engineering, College of Environment and Natural Resources, Can Tho University, Can Tho City 900000, Vietnam

[9] Faculty of Environmental Earth Science, Hokkaido University, Sapporo 060-0810, Japan

[10] Department of Civil Engineering, Chennai Institute of Technology, Chennai 600069, Tamilnadu, India

[11] Center of Excellence for Climate Change Research/Department of Meteorology, King Abdulaziz University, Jeddah, Saudi Arabia